PROTECTIVE AND FUNCTIONAL POWDER COATINGS

QUALITY ANALYSIS OF ALUMINIZED SURFACE LAYERS PRODUCED BY ELECTROSPARK DEPOSITION

**G. V. Kirik,[1] O. P. Gaponova,[2,6] V. B. Tarelnyk,[3]
O. M. Myslyvchenko,[4] and B. Antoszewski[5]**

UDC 621.9.048

The structurization of aluminum coatings on steel 20 and 40 substrates produced in different ESD modes is considered. The thickness and microhardness of 'white' and transition layers and the surface roughness increase and chemical and phase compositions change with higher discharge energy. The coating formed at low discharge energies mainly consists of α-Fe and aluminum oxides. Electron microprobe analysis shows that the coating produced at high discharge energies consists of iron and aluminum intermetallics and free aluminum. Compared to steel 20, the electrospark-deposited coating on steel 40 has a deeper layer with increased hardness and has greater microhardness. The surface roughness remains virtually the same. To decease roughness and increase integrity of the coatings, we recommend electrospark deposition with the same electrode (aluminum), but at lower discharge energies (W_d = 0.52 J).

Keywords: electrospark alloying, aluminizing, microstructure, coating, surface, X-ray diffraction, electron microprobe analysis, microhardness, surface roughness.

INTRODUCTION

One of the most challenging aspects in technological progress is that the properties of new materials used in mechanical engineering must constantly comply with tougher performance conditions. Generally, at least one parameter of these materials fails to meet the requirements. The material surface is most often the weakest element in the 'material–operating environment' system, determining allowed performance conditions and lifetime of the entire system. This indicates that the development of techniques and processes for depositing protective coatings is of great importance. The deposition of coatings onto materials for high-temperature applications is required because the parts cannot achieve better performances even if they are made of new materials possessing improved physical, mechanical, and metallurgical properties.

The choice of a specific coating in the above system is determined by the balance between the results and costs, i.e., the ratio between the improvement in performances of a part and the cost of depositing a coating onto this part.

[1]UKRROSMETAL Concern, Sumy, Ukraine. [2]Sumy State University, Sumy, Ukraine. [3]Sumy National Agrarian University, Sumy, Ukraine. [4]Frantsevich Institute for Problems of Materials Science, National Academy of Sciences of Ukraine, Kyiv, Ukraine. [5]Kielce University of Technology, Kielce, Poland.

[6]To whom correspondence should be addressed; e-mail: gaponova@pmtkm.sumdu.edu.ua.

Modern technology offers various methods to measure the physicochemical and performance characteristics of metallic surfaces for a given application, each of these methods having its optimum applications. Electrospark deposition (ESD) belongs to economical and resource-saving methods of surface hardening and applying protective coatings. Its advantages are as follows: any conductive material as a compact electrode can be deposited onto the surface of interest; the layer applied exhibits high adhesion to the base material; the process does not require much energy; the operations are simple; the process is highly effective, etc. [1].

Aluminizing is known [2] to be used to increase the oxidation resistance, atmospheric corrosion resistance, and a series of other properties possessed by iron–carbon alloys. In addition, there has been a recent trend to use ESD to apply complex aluminized coatings to serve as protective and wear-resistant layers [3, 4], characterized by high melting point, low density, high elastic modulus, and adequate creep resistance, oxidation resistance, and ignition resistance. Hence, to examine the quality of ESD-aluminized coatings is an important task.

The objective of this research effort is to improve the performances of parts made of structural carbon steels by aluminizing their surfaces applying ESD, being an economical and environmentally friendly method.

EXPERIMENTAL PROCEDURE

The substrates were 15 mm × 15 mm × 8 mm samples made of steel 20 and 40 (as per GOST 1050–88); aluminum coatings were deposited on these substrates with ESD employing an Elitron-52A unit with a hand-held vibrator. The electrodes were rods made of SvA99 aluminum wire (as per GOST 7871–75) 4 mm in diameter and 45 mm in length.

The deposition process included five modes with different discharge energies W_d and discharge rates—coating area formed per unit time (Table 1). When the ESD rate reduces, quality of the surface layer deteriorates—burn marks show up and the layer being formed fails—which is especially evident in 'rougher' modes (at $W_d > 1$ J) [1]. In turn, higher deposition rates affect the coating integrity.

TABLE 1. ESD Modes

Mode	W_d, J	Deposition rate, cm^2/min
1	0.52	1.0–1.3
2	1.30	1.3–1.5
3	2.60	1.5–2.0
4	4.60	2.0–2.5
5	6.80	2.5–3.0

Metallographic analysis of the coatings was carried out using a MIM-7 optical microscope (LOMO, USSR) and a JSM 7100f electrical microscope (JEOL Ltd., Japan), and their hardness was determined with a PMT-3 tester. X-ray diffraction was conducted in Cu-K_α radiation employing a PROTO AXRD diffractometer (PROTO Manufacturing Inc., USA) equipped with a silicon point detector (SPD). The X-ray diffraction patterns were plotted through point-by-point scanning. The scan angle was 0.05° and exposure time at one point was 2 sec. The experimental results were processed with the Powdercell 2.4 software for full-profile analysis of X-ray diffraction patterns for a polycrystalline phase mixture. Since the peaks were multiphase and a number of peaks overlapped, they were separated by fitting to the Pseudo-Voigt 2 function. The least-squares method was used to reach the best agreement between the experimental and fitted patterns considering the double nature of Cu-K_α radiation.

Electron microprobe analysis of the ESD coating involved recording of characteristic X-rays induced by the electron beam of the chemical elements present in microvolume. For this analysis, an electron microscope equipped with an ISIS 300 microanalyzer (Oxford Instruments, Great Britain) was employed.

The surface roughness after ESD was determined by plotting and processing the surface profiles using a model 201 roughness meter (Kalibr Instrument Plant, Moscow, Russian Federation).

Figure 1 shows the microstructure of an aluminum layer on steel 20 depending on discharge energy W_d. Metallographic analysis indicates that the coating microstructure is presented by three regions: 'white' layer, which cannot be etched by ordinary etchants; transition or diffusion zone; and base metal, with ferrite–pearlite structure. Table 2 presents sizes of the layers versus discharge energy.

Electrospark deposition in mode 1 (Table 1) produces a thin transition layer 20–30 μm thick, whose integrity tends to reach 100%. There are individual 'white' layer regions (up to 60%) 10–12 μm thick. The 'white' and transition layers become thicker with increasing discharge energy. The 'white' and transition layers are 30–50 and 30–40 μm at $W_d = 1.30$ J and 50–70 and 40–60 μm at $W_d = 4.60$ (Table 2). The surface layer displays better integrity with tougher ESD mode. Thus, the diffusion zone tends to reach 100% integrity and the 'white' layer 85% integrity at $W_d = 2.60$ J (mode 3).

Figure 2 shows how microhardness is distributed in the samples with depth from the surface according to hardness testing. The maxim hardness is reached on the sample surface and smoothly decreases to the substrate microhardness (1600–1700 MPa). The microhardness of coating layers is determined by ESD energy parameters:
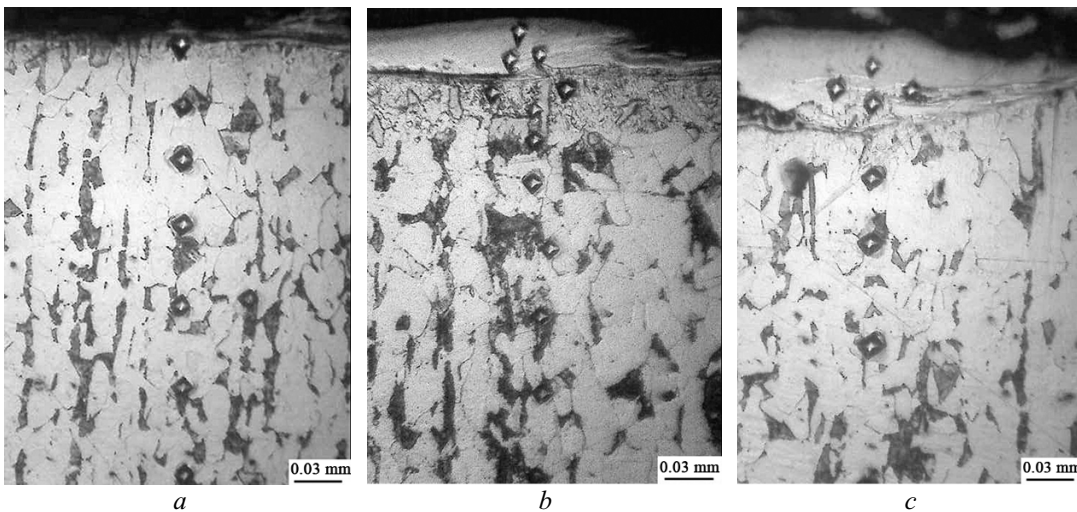

Fig. 1. Cross-structural microstructure of the aluminum-coated steel 20 samples produced by ESD in modes 1 (*a*), 2 (*b*), and 3 (*c*)

TABLE 2. Qualitative Parameters of Aluminized Electrospark-Deposited Coatings on Steel

| W_d, J	Thickness, μm		Microhardness H_μ, MPa		Roughness, μm			'White' layer integrity, %
	'White' layer	Transition layer	'White' layer	Transition layer	R_a	R_z	R_{max}	
Steel 20								
0.52	10–12	20–30	2000 ± 70	1900 ± 50	1.3	2.3	9.3	60
1.30	30–50	30–40	2050 ± 70	1850 ± 80	1.9	6.2	21.6	80
2.60	40–50	30–50	2700 ± 70	2000 ± 200	3.3	9.3	23.2	85
4.60	50–70	40–60	5010 ± 90	2250 ± 200	6.2	16.3	40.6	95
6.80	to 70	110–130	7270 ± 50	2370 ± 70	9.0	18.1	58.3	100
Steel 40								
0.52	10–15	10–20	2350 ± 50	2000 ± 50	1.6	3.0	8.1	50
2.60	30–70	30–70	3500 ± 50	4500 ± 50	1.9	4.1	11.6	70
6.80	60–130	130–150	7400 ± 70	2390 ± 70	8.1	17.3	49.0	100
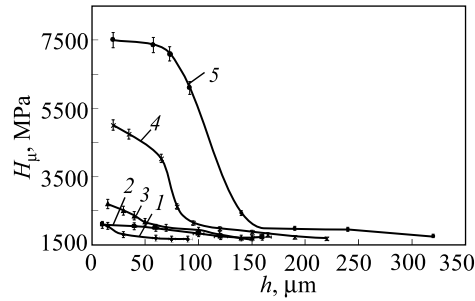
Fig. 2. Microhardness H_μ versus depth h of the coating on the steel 20 samples produced by ESD in modes 1–5

the higher the discharge energy, the harder is the 'white' layer and, thus, the transition layer. This change in the microhardness seems to be due to the diffusion of aluminum into the substrate and variation in the coating phase composition.

Analysis of the Fe–Al phase diagram indicates [7] that intermetallics can form in the electrospark-deposited coating (which is ascertained by its high hardness). The formation of nitrides and oxides cannot be excluded either [8] since the coating was deposited in air. Small amounts of the pure electrode material are very likely to be observed.

The phase composition of the ESD coatings was determined by X-ray diffraction. The X-ray diffraction patterns (Fig. 3) were plotted for the sample being aluminized in mode 1 (Table 1). They show diffraction peaks of two solid solutions formed by a bcc phase, α-Fe and α-Fe' (229 space group), and aluminum oxide γ-$Al_{2.67}O_4$ (227 space group). The α-Fe and α-Fe' phases differ only in the lattice parameter, which seems to result from macrostresses induced by rapid cooling after ESD (Table 3).

New phase components appear with increasing discharge energy. While only a solid solution of aluminum in iron and a small amount of aluminum oxide (since ESD proceeds in air) show up in mode 1 (Tables 1 and 3), a
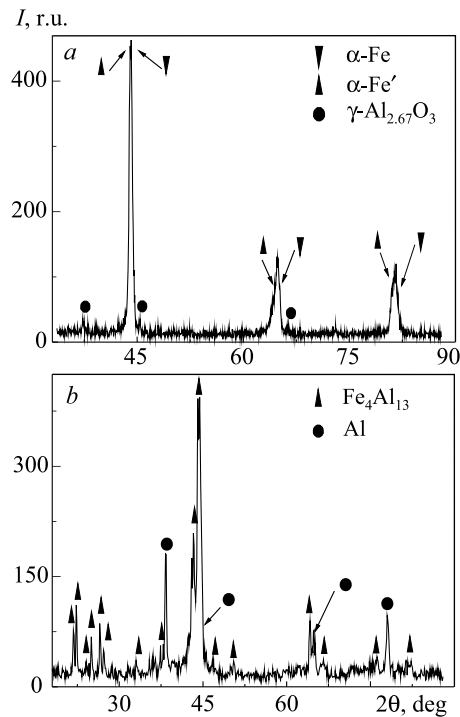

Fig. 3. X-ray diffraction patterns for the steel 20 surface produced by ESD with aluminum in modes 1 (*a*) and 2 (*b*)

TABLE 3. Lattice Parameters and Quantitative Analysis of the Phases after Aluminizing

Mode	Phase	Lattice parameters	Phase content, wt.%
1	α-Fe	$a = 0.2887$ nm	36
	α-Fe'	$a = 0.2907$ nm	47
	γ-Al$_{2.67}$O$_4$	$a = 0.7980$ nm	17
2	Al	$a = 0.4056$ nm	19
	Fe$_4$Al$_{13}$	$a = 1.5403$ nm, $b = 0.8134$ nm, $c = 1.2473$ nm, $\beta = 108°$	81

monoclinic Fe$_4$Al$_{13}$ phase (space group 12) and pure aluminum (space group 225) can form in mode 2. The formation of intermetallic phases apparently promotes higher coating hardness and discharge energy (Fig. 2).

Like in the papers [9, 10], we took the Mo–Fe and Cu–Fe pairs to show that higher discharge energy increases thickness of the coating and diffusion zone in interaction of aluminum with iron (steel) in air. The aluminum–iron diffusion zone in the samples produced in modes 1 and 2 is 34 and 50 μm thick, respectively (Fig. 4). Note that the amount of aluminum in iron increases as well: a thin layer (to 4 μm), containing ~1.5–2 times more aluminum, forms at $W_d = 1.30$ J on the sample. The presence of free aluminum in the layer is confirmed by X-ray diffraction (Table 3).
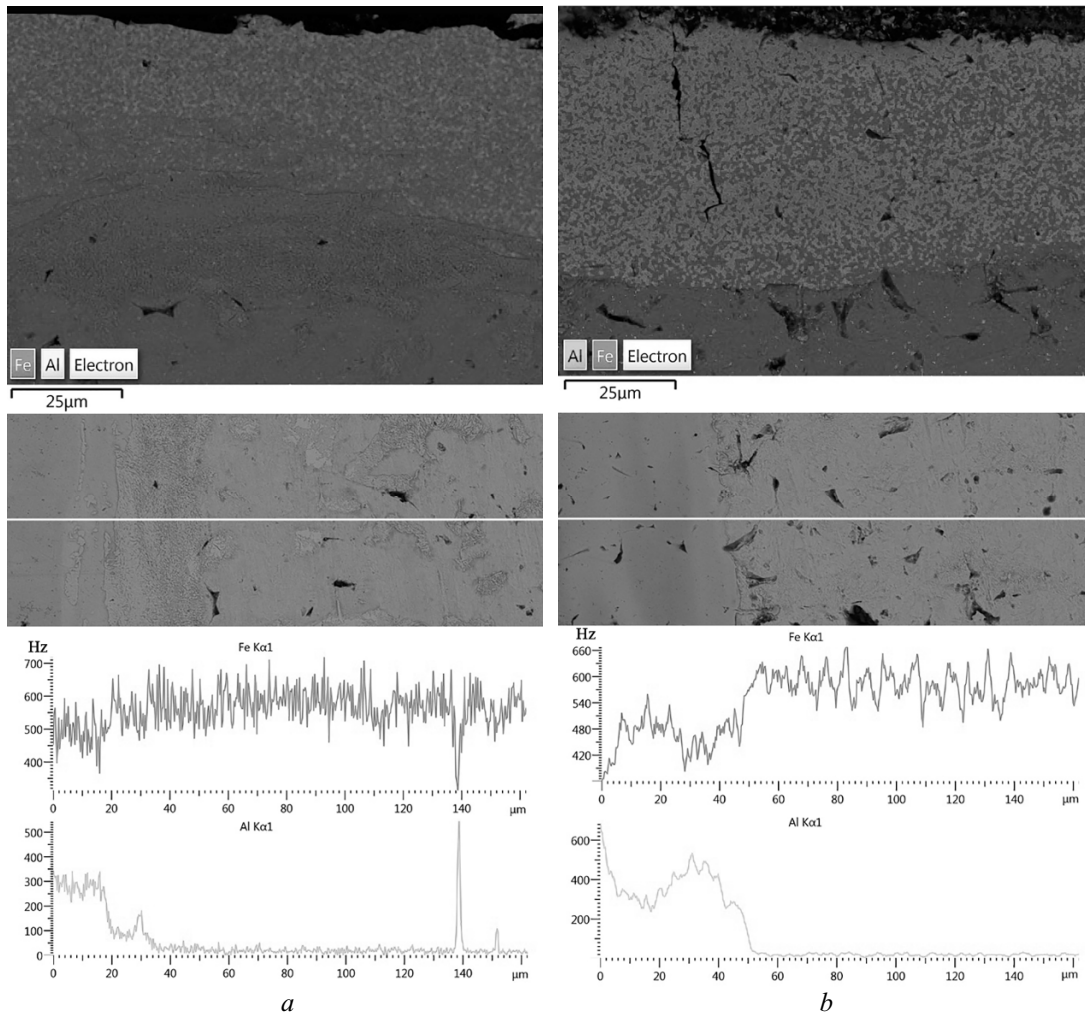

Fig. 4. Composition curves showing distribution of iron and aluminum in the coating produced by ESD in modes 1 (*a*) and 2 (*b*)
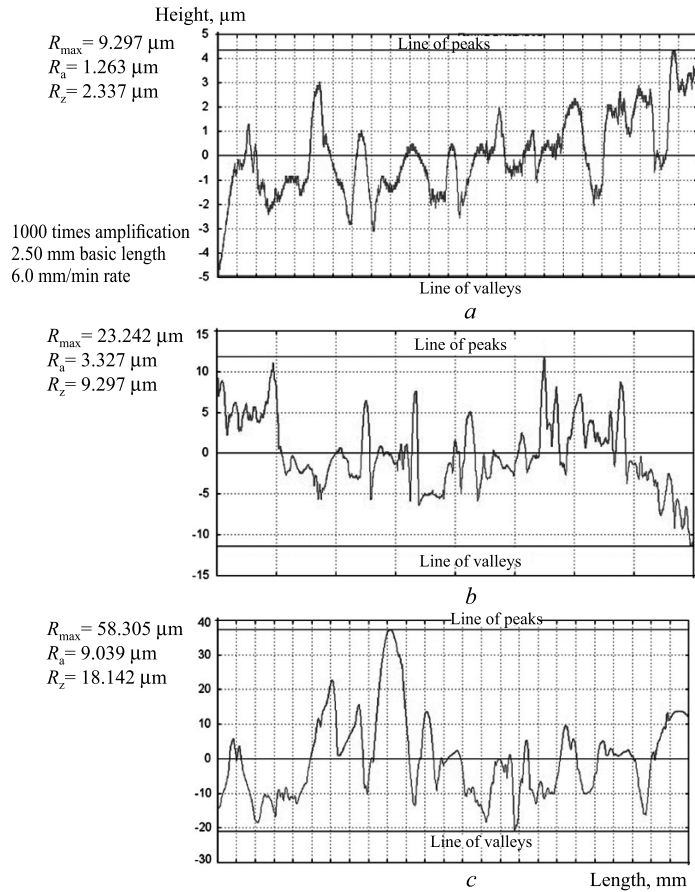
Fig. 5. Surface roughness profiles of the steel 20 samples after ESD with aluminum in modes 1 (*a*),
3 (*b*), and 5 (*c*)

Surface analysis of the steel 20 sample aluminized with ESD shows that its roughness increases with discharge energy (Table 2): $R_a = 1.3$ μm at $W_d = 0.52$ J and $R_a = 3.3$ μm at $W_d = 2.60$ J. Further increase in discharge energy to 6.8 J is accompanied by significant increase in roughness: $R_{max} = 58.305$ μm, $R_a = 9.039$ μm, and $R_z = 18.142$ μm (Fig. 5).
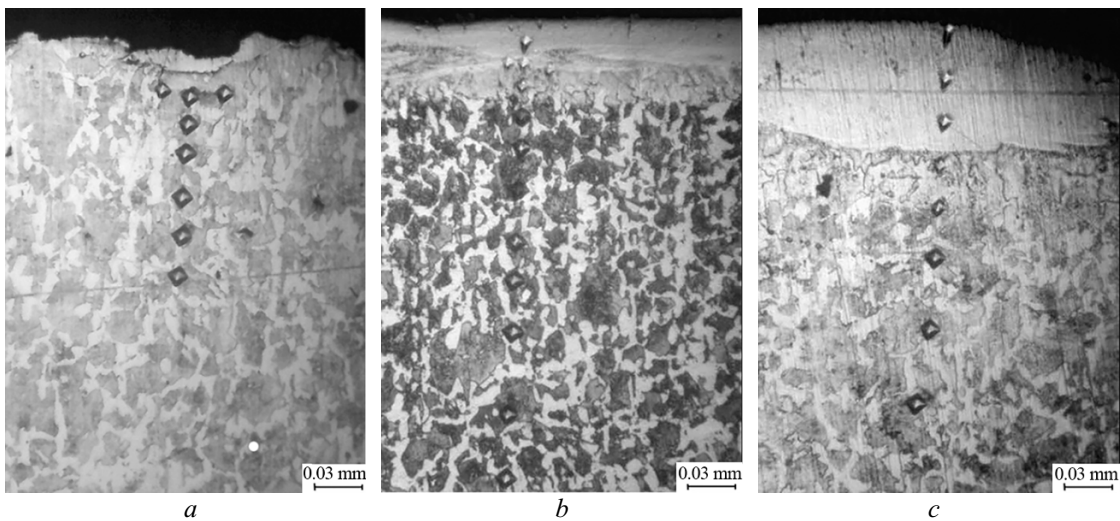

Fig. 6. Cross-sectional microstructure of the steel 40 samples with the aluminum coating produced by ESD in modes 1 (*a*), 3 (*b*), and 5 (*c*)
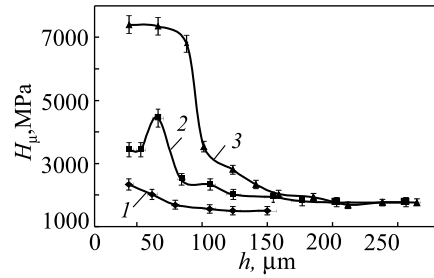
Fig. 7. Microhardness H_μ versus depth h of the coating on the steel 40 samples produced by ESD in modes 1 (*1*), 3 (*2*), and 5 (*3*)

Metallographic analysis of the coatings on steel 40 indicates that they consist of three layers like those on steel 20 (Fig. 6). Note that layers of greater thickness and higher microhardness form on steel 40, the ESD conditions being equal (Fig. 7). Thus, the 'white' layer is 30–70 μm thick and has $H_\mu = 3500 \pm 50$ MPa on steel 40 and is 40–50 μm and has $H_\mu = 2700 \pm 70$ MPa on steel 20 after ESD in mode 3. As discharge energy increases, the 'white' layer displays higher integrity, and that of the transition layer tends to 100% (Table 2).

The transition layer becomes deeper with higher discharge energy in ESD: this is not evident at $W_d = 0.52$ J, while it is about 30–40 μm thick and has increased hardness (~4500 MPa) at $W_d = 2.60$ J. The transition layer hardness may increase because of phase transformations that occur when steel is heated above critical temperatures and because of accelerated cooling in air. The microstructure displays an incomplete recrystallization region, which is determined by heating to 730–755ºC for steel 40. This metal region is subjected only to partial recrystallization:
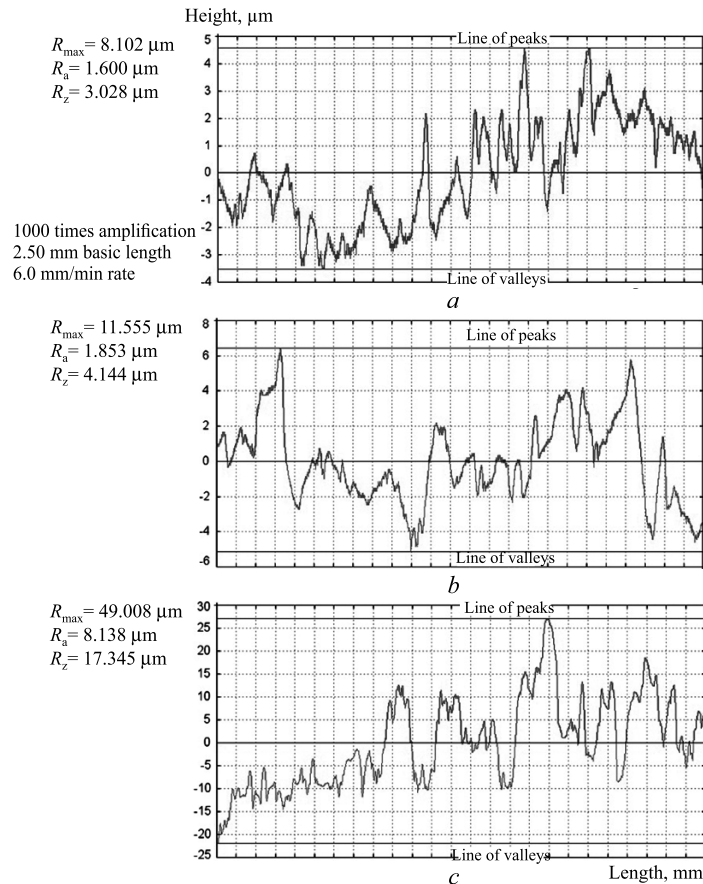

Fig. 8. Surface roughness profiles for the steel 40 samples after ESD with aluminum in modes 1 (*a*), 3 (*b*), and 5 (*c*)

$R_{max} = 9.297\ \mu m$
$R_a = 1.263\ \mu m$
$R_z = 2.337\ \mu m$

Height, μm

Line of peaks

1000 times amplification
2.50 mm basic length
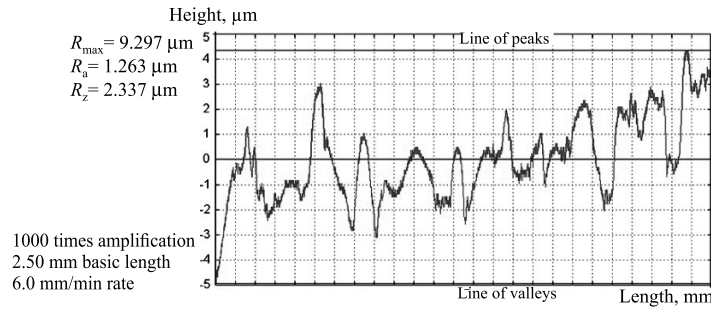6.0 mm/min rate

Line of valleys

Length, mm

Fig. 9. Surface roughness profile for the steel 20 sample after successive aluminizing with ESD in modes 2 and 3

TABLE 4. Rate (cm^2/min) of Electrospark Deposition of Carbon and Aluminum onto Aluminized Steel Samples

Mode	ESD with aluminum	ESD with graphite electrode
1	0.8–1.0	0.5–0.7
2	1.0–1.2	0.7–1.0
3	1.3–1.5	1.0–1.2
4	1.6–1.8	1.2–1.5

there are both starting metal grains and newly formed grains. In spite of the accelerated cooling of steel 40 after ESD in air (because of small resistance of overcooled austenite), acicular (martensitic) structure does not form. Note that martensite may cause cracking as it has high hardness and brittleness. It can be assumed that the surface layer still has small strain despite increase in hardness. Moreover, intermetallics, nitrides, and oxides may form in the steel 40 surface layer as ESD proceeds in air, which is the case for steel 20. This significantly increases microhardness of the coating and transition layer. Surface analysis of the steel 40 samples after ESD with aluminum shows that their roughness increases with discharge energy. At $W_d = 0.52$ J, $R_{max} = 11.555\ \mu m$ and average roughness values are $R_a = 1.853\ \mu m$ and $R_z = 4.144\ \mu m$ (Fig. 8). Therefore, the qualitative parameters such as thickness, roughness, and microhardness of the 'white' and transition layers increase with discharge energy in ESD of an aluminum electrode onto steels 20 and 40 (Table 2). The 'white' layer integrity is low, 50–60%, at $W_d = 0.52$ J and increases to 100% when discharge energy becomes $W_d = 6.8$ J.

To decrease the roughness of electrospark-deposited coatings, the paper [11] proposes soft deposition of graphite as the final operation (after the main deposition process). In this case, a diffusion layer rather than a graphite layer forms. The cathode metal is ejected where pulses are applied, i.e., the most protruding surface parts are sputtered. This smoothens the ridges, and surface roughness decreases.

To reduce surface roughness after ESD with an aluminum electrode, we propose the use of the same electrode (aluminum) but lower discharge energies in subsequent treatment. The electric discharge is applied in this case between the surface roughness peaks and aluminum electrode; as a result, the peaks collapse and surface roughness decreases. In our previous studies [12, 13], we showed the effectiveness of this ESD process.

Table 4 shows the rate of electrospark deposition of carbon (graphite electrode) and aluminum onto aluminized steel samples depending on the discharge energy.

Figure 9 shows surface roughness of the steel 20 sample aluminized with ESD first with $W_d = 2.6$ J at a rate of 1.8 cm^2/min and then with $W_d = 1.3$ J at a rate of 0.8 cm^2/min. We can see than surface roughness is decreased: $R_{max} = 9.297\ \mu m$, $R_a = 1.263\ \mu m$, and $R_z = 2.337\ \mu m$.

CONCLUSIONS

The structurization of aluminum coatings on steel 20 and 40 produced in different ESD modes has been considered. The coating consists of three regions: 'white' layer, diffusion zone, and base metal. The thickness and

microhardness of the 'white' layer and transition zone and the surface roughness increase with discharge energy. Integrity of the 'white' layer is low (50–60%) at $W_d = 0.52$ J and increases to 100% at $W_d = 6.8$ J. Increase in the ESD discharge energy changes the chemical and phase composition. The layer mainly consists of α-Fe and aluminum oxides at low discharge energies and of iron and aluminum intermetallics and free aluminum at higher discharge energies.

We have compared the effect of substrates on the properties of surface layers produced by ESD in different modes: when steel 20 is replaced by steel 40, the 'white' and transition layers become thicker (i.e., increased hardness zone deepens), and surface layer microhardness increases. The surface roughness remains virtually the same.

For applications we can recommend aluminizing with ESD in modes 4 and 5 ($W_d = 4.6$–6.8 J and 2.0–3.0 cm^2/min rate) to produce the 'white' layer 70–130 μm thick with $H_\mu = 5000$–7500 MPa, $R_a = 6$–9 μm, and 95–100% integrity.

To decrease surface layer roughness and ensure coating integrity, we recommend ESD with the same electrode (aluminum), but at lower discharge energies.

REFERENCES

1. A. E. Gitlevich, V. V. Mikhailov, N. Ya. Parkanskii, and V. M. Revutskii, *Electrospark Deposition of Metallic Surfaces* [in Russian], Stiintsa, Kishinev (1985), p. 196.
2. V. R. Ryabov, *Steel Aluminizing* [in Russian], Metallurgiya, Moscow (1973), p. 240.
3. S. A. Pyachin and A. A. Burkov, "Production of intermetallic coatings by electrospark deposition of titanium and aluminum onto steel substrate," *Elektron. Obrab. Mater.*, **51**, No. 2, 16–23 (2015).
4. V. I. Agafii, V. A. Yurchenko, V. I. Yurchenko, et al., "Wear resistance of coatings produced by electrospark deposition of Al–Sn alloy electrodes," *Elektron. Obrab. Mater.*, **47**, No. 6, 12–16 (2011).
5. C. Leyens, M. Peters, and W. A. Kaysser, "Intermetallic Ti–Al coatings for protection of titanium alloys: oxidation and mechanical behavior," *Surf. Coat. Technol.*, **94–95**, 34–40 (1997).
6. X. Wu, "Review of alloy and process development of TiAl alloys," *Intermetallics*, **14**, 1114–1122 (2006).
7. O. A. Bannykh, P. B. Budberg, S. P. Alisova, et al., *Phase Diagrams of Binary and Multicomponent Iron Systems: Handbook* [in Russian], Metallurgiya, Moscow (1986), p. 440.
8. Yu. I. Mulin and A. D. Verkhoturov, *Electrospark Deposition of Electrode Produced from Mineral Raw Materials onto Effective Surfaces of Tools and Machine Parts* [in Russian], Dal'nauka, Vladivostok (1999), p. 110.
9. D. S. Gertsriken, V. F. Mazanko, Q. Shengru, et al., "Interaction of nickel and molybdenum with air gases under spark discharges," in: *Proc. 50th Int. Sci. Symp. Current Problems of Strength* [in Russian], Vitebsk. Gos. Tekhnol. Univ., Vitebsk, Belarus (2010), Part. 1, pp. 164–167.
10. V. F. Mazanko, D. S. Gertsriken, V. M. Mironov, et al., "Interaction of aluminum with iron and air gases in electrospark deposition," in: *Proc. 11th Int. Conf. Interaction of Radiation with Solids* [in Russian], Minsk, Belarus (2015), pp. 240–242.
11. V. B. Tarelnik (ed.), B. Antoszewski, V. S. Martsinkovskii, et al., *Cementation by Electrospark Deposition: Monograph* [in Russian], University Book, Sumy (2015), p. 220.
12. V. S. Martsinkovskii, V. B. Terelnik, and M. P. Bratushchak, *Method for Cementation of Steel Parts by Electrospark Deposition* [in Russian], Russian Federation Patent 2468899, IPC B 23H 9/00, Bulletin No. 34, publ. December 10 (2012), p. 11.
13. V. S. Martsinkovskii, V. B. Terelnik, and M. P. Bratushchak, *Method for Cementation of Steel Parts by Electrospark Deposition* [in Ukrainian], Ukrainian Patent 101715, IPC 23H 9/00, Bulletin No. 8, publ. January 25 (2013), p. 9.